

On-Site Radiated Emissions Result Visualization Using Augmented Reality

Denys Pokotilov^{ID}, Robert Vogt-Ardatjew^{ID}, *Member, IEEE*, and Frank Leferink^{ID}, *Fellow, IEEE*

Abstract—By focusing on regions exhibiting maximum electromagnetic (EM) emission levels, the duration required for standard EM emissions measurements can be substantially reduced. This letter outlines a rapid prescan technique that adheres to conventional measurement procedures. The proposed method considerably minimizes measurement time by identifying areas where emissions approach, or exceed, threshold limits. Furthermore, real-time visualization of EM emissions from the time-domain data enables testers to select a more effective scanning trajectory, thus diminishing the likelihood of overlooking areas with high-intensity EM emissions and time-variance sources.

Index Terms—Augmented reality (AR), electromagnetic compatibility (EMC), high-level EME areas localization, radiated EM field visualization, time domain.

I. INTRODUCTION

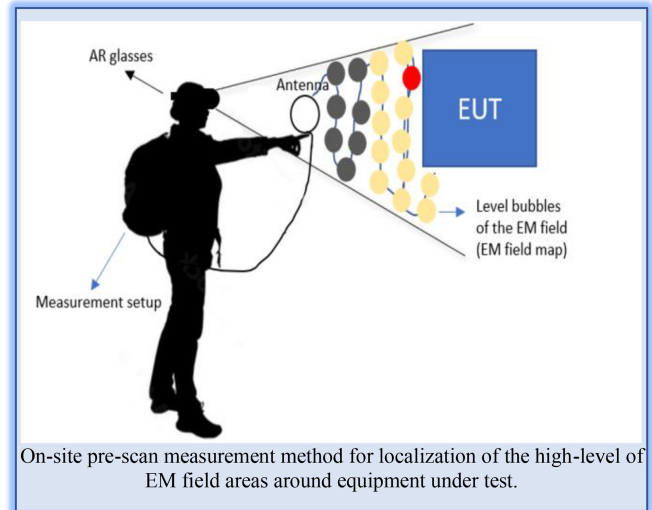
RADIATED emissions testing, as detailed in AECTP 501 [1], ANSI C63.4 [2], and CISPR 16-1-4:2019 [3], necessitates exhaustive measurements across the entire test area from various spatial positions. Standard measurement procedures, such as those in AECTP 501, NRE01, and applied to a one-side surface of 1 m², can take around 2 h to complete in the frequency domain [1]. This long measurement time can be attributed to two main factors: 1) frequency-domain measurements in the low-frequency range and 2) the vast number of measurement positions above the surface. It is important to note that operational mode changes can cause significant variations over time in the radiation spectrum and amplitude. If measurements are taken between pulses, for instance, peak radiated emissions might be grossly underestimated. The shift toward variable sources and loads like switched-mode power supplies (SMPSs) emphasizes the increasing importance of time-domain information acquisition, especially considering power efficiency [4]. To mitigate the first time-consuming factor, time-domain measurements can be employed [5], [6], [7]. In this regard, a 1-min standard measurement above the

Manuscript received 22 May 2023; revised 22 August 2023; accepted 3 October 2023. Date of publication 12 October 2023; date of current version 17 November 2023. This work was supported by the European Union's Horizon 2020 Research and Innovation Programme under the Marie-Sklódowska-Curie Grant under Agreement 812753. (*Corresponding author: Denys Pokotilov.*)

Denys Pokotilov and Robert Vogt-Ardatjew are with the Department of EEMCS, University of Twente, 7522 NB Enschede, The Netherlands (e-mail: denys.pokotilov@utwente.nl).

Frank Leferink is with the Department of EEMCS, University of Twente, 7522 NB Enschede, The Netherlands, and also with Thales Nederland B.V., 7554 RR Hengelo, The Netherlands (e-mail: frank.leferink@utwente.nl).

Digital Object Identifier 10.1109/LEMCPA.2023.3324267



antenna position would yield a 0.15-s data recording in the time domain which is equivalent to the longest dwell time for a frequency step, thereby drastically reducing measurement time. However, the primary time-consuming part remains as the sheer number of spatial measurement points, as the antenna must physically be moved for every position.

To reduce the amount of measurement positions, a fast prescan method with peak detector implementation can be utilized. This allows for the detection of high electromagnetic (EM) field areas and significantly reduces the total measurement positions above the surface [4].

Several studies have suggested antenna tracking methods over the measurement area to identify high-emission spots [8], [9], [10], [11]. These methods enable the creation

Take-Home Messages:

- The pre-scan approach streamlines standard evaluation procedures, improving efficiency and cost-effectiveness.
- Customizable measurement equipment ensures relevance to current industry standards.
- Three-dimensional map of measured emissions provides a comprehensive and accurate representation of EM emissions levels.
- The proposed method can detect multiple high-level EME areas/sources, enabling effective and precise mitigation strategies.
- The AR glasses provide real-time visual feedback of the measurement results, displaying the data on the glasses' screen in a timely manner.

of an EM emission map above the scanned surface, offering additional information about the equipment under test (EUT) and reducing the likelihood of underestimating high-level EM emission areas. However, these methods are often under-utilized due to the prerequisite that the antenna tracking system should not interfere with measurement results. As such, data sources, like laptops, are kept at a distance to prevent disruption.

In [12], video tracks were shown to be the optimal method for antenna tracking in this context. However, video tracking faces limitations in hardware (camera quality) and software (pattern recognition) and can be challenging to implement (camera position). As a solution, the use of augmented reality (AR) glasses, which integrate the tracking system seamlessly and enhance radiated EM emission measurements, is proposed. AR, an innovative technology that combines virtual images with real-world perception, is becoming increasingly prevalent across various sectors, thanks to advanced high-performance computing systems [12].

AR glasses, equipped with a depth sensor and four cameras, can track the antenna in three dimensions, offering accurate tracking data even for small distances [9]. This enables precise EM emission measurements over complexly shaped areas. By using AR glasses, several issues are resolved: independence of the antenna tracking method from the camera position, real-time measurement results visualization, and the possibility of using a portable digitizer for data acquisition via a fast prescan method. The usability of the digitizers for the time-domain measurements was shown in [4].

Employing a combination of a digitizer, laptop, and AR glasses allows swift identification of high EME areas by moving the antenna around the EUT or the measured area. The proposed method utilizes a standard NRE01 13-cm shielded loop antenna and complies with standard requirements, including the required dwell time for the longest frequency step measurement. Standard requirement implementation, such as antenna type, detector, and frequency step for postprocessing, enhances the prescan measurement procedure, aligning it more closely with the standard measurement process. The AR glasses continually record the antenna position, and real-time data processing on the laptop generates an emission map, which is displayed on the glasses' screen.

II. MEASUREMENT SETUP AND METHOD

The measurement setup is depicted in Fig. 1. The tracking component is performed by a HoloLens device that employs a depth sensor in conjunction with four cameras capable of understanding the environment to track the object in three dimensions (X, Y, Z). In order to accommodate various antenna constructions, the proposed object-tracking method is linked to the human hand holding the antenna. Digitized data acquisition is carried out using the PicoScope™ 5000 series [13], which streams the data to a laptop where postprocessing is executed. The postprocessing is performed by a custom script, utilizing the FFTW library, which enables the manual selection of step frequency, resolution bandwidth, and peak and average detectors. A shielded



Fig. 1. Measurement setup.

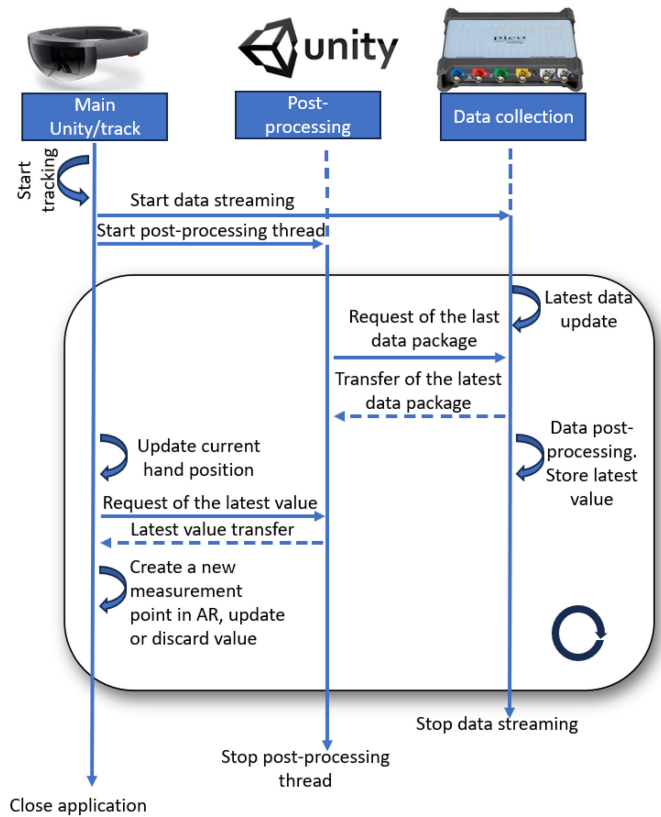


Fig. 2. Sequence diagram of the process thread during the measurement.

loop antenna was utilized to measure the magnetic field in accordance with NRE01 [1]. The frequency of interest of this test method is 30 Hz–100 kHz.

The system is developed in the Unity game engine and operates on a laptop that streams the visualization to the HoloLens through Wi-Fi. The use of Wi-Fi is preferred as it does not affect low-frequency measurements. However, a wired connection between the laptop and AR glasses is also available to minimize interference in high-frequency measurements (Fig. 2).

A sequence diagram of the main process is depicted in Fig. 2. The system utilizes three distinct threads: one for data collection, one for data postprocessing, and one for visualizing the measurement results.

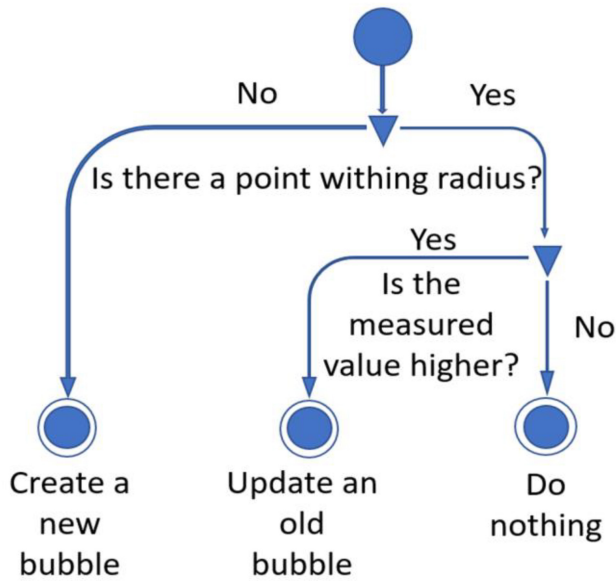


Fig. 3. Diagram of the AR bubbles updates.

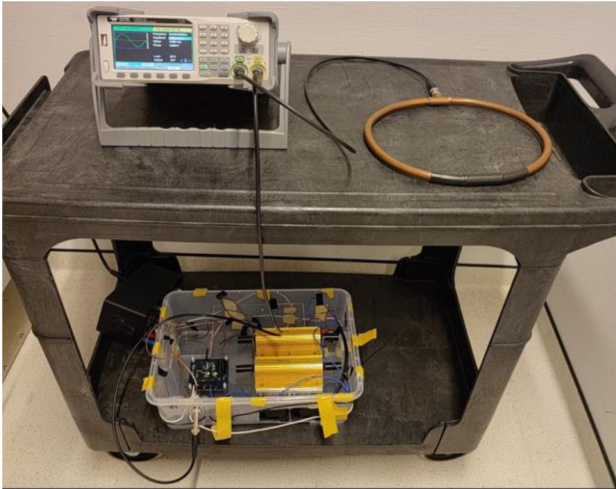


Fig. 4. EUT: signal generator, stable emission source (antenna), and pulse emission source (bottom).

The visualization thread is responsible for tracking and the logic of the Unity Engine. The data collection thread continuously streams data, while the postprocessing thread retrieves the latest package of TD data each time it completes processing the previous package. The tracking thread retrieves the latest calculated value from the postprocessing thread after each measurement point is made. An activity diagram of measurement point creation in AR can be seen in Fig. 3. To ensure that high-emission levels from nonstable emission sources are not missed when returning to a previously tested area, the latest calculated value is compared to neighboring visualized measurement points. The highest value at that location will be overwritten and visualized. The visualization of the highest measured EM field level in AR depends on the time for data package creation, which in this case was 0.3 s, which is related to the longest measurement time of the single-frequency component in FD. The EUT is illustrated in Fig. 4 [5]. A shielded

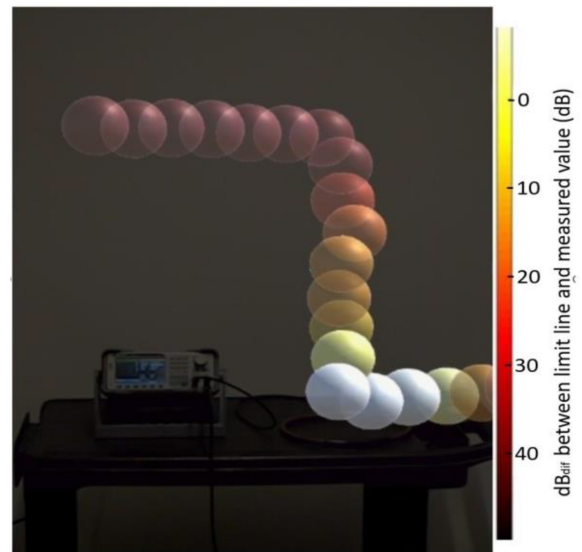


Fig. 5. Measurement result changes with closer proximity to the area with a high EMI level (white bubbles nearest measurement to the transmitting antenna).

loop antenna was connected to a signal generator to simulate a stable emission source, while a half-bridge evaluation board driven by a signal generator was used at the bottom to mimic a nonstable emission source [8]. This EUT was utilized to demonstrate the ability to recognize multiple high-emission areas located near one another.

III. MEASUREMENT RESULTS

The representation of 3-D measurement results in a paper can be challenging. To depict what the tester observes during real-time measurements, 2-D figures are utilized in this letter, as illustrated in Fig. 5. The experiment shown in Fig. 5 involves a transmitting loop antenna, which creates an area with a high EM field. The figure shows a clear spatial pattern, with the calculated maximum value increasing as the receiver antenna approaches the emitting spot. Fig. 5 illustrates one of the most significant benefits, which is the visualization of EME distribution from the emission source. This enables advantageous postprocessing to analyze high-level emission areas/equipment and implement measures to mitigate or eliminate EME. The complete spectrum calculated during the measurements, tied to the antenna position, can be extracted from the code. However, in this letter, the largest difference between the measured value and the limit line, represented by Dif, is used to indicate high- or low-emission areas.

Dif is the maximum value in dB over the frequency range, while $\text{dBlim}(f)$ and $\text{dBmeas}(f)$ represent the value of the standard limit line in dBpT and the postprocessed value from TD measurements in dBpT over the frequency range, respectively. For the standard NRE01, one data block was recorded over 0.15 s, which represents the minimum measurement time for the frequency step. Fig. 6 shows peak prioritization over the whole frequency range according to the limit line for each recorded data block. The spectra in Fig. 6 are discontinuous

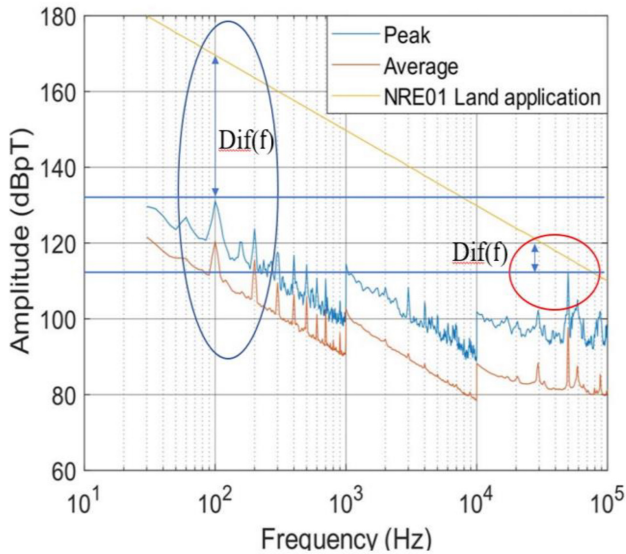


Fig. 6. Peaks prioritization on the frequency range according to the limit line.

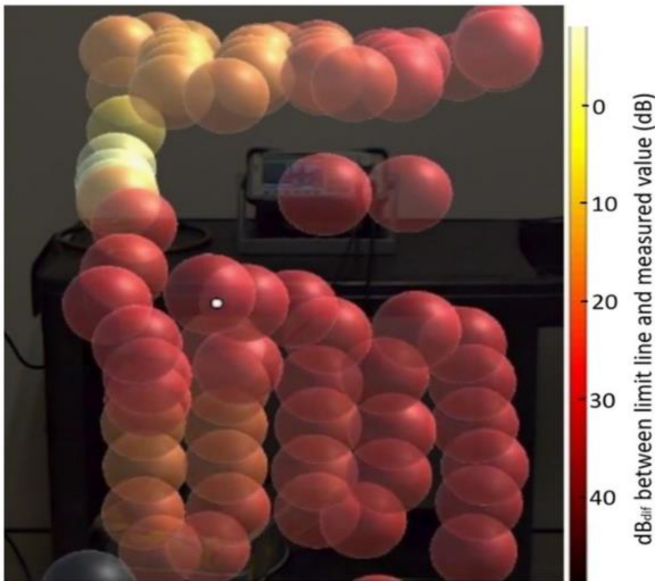


Fig. 7. High-level areas measurements with several emission sources.

because, as prescribed in the standard, they are calculated with different IF bandwidths for three frequency subranges. It is clearly visible that the peak which is at the frequency of 100 Hz is even higher than the peak at 50 kHz, but due to the limit line, 50 kHz will be the main priority since it is closest to the limit line

$$Dif = dB_{meas}(f) - dB_{lim}(f). \quad (1)$$

The color representation of the emission measurement was chosen to range from black to white, where black represents the lowest emission levels (below the limit line) and white represents the highest emission levels (near or above the limit line) [1]. Fig. 7 depicts the measurement results obtained using the proposed method in the vicinity of several emission sources.

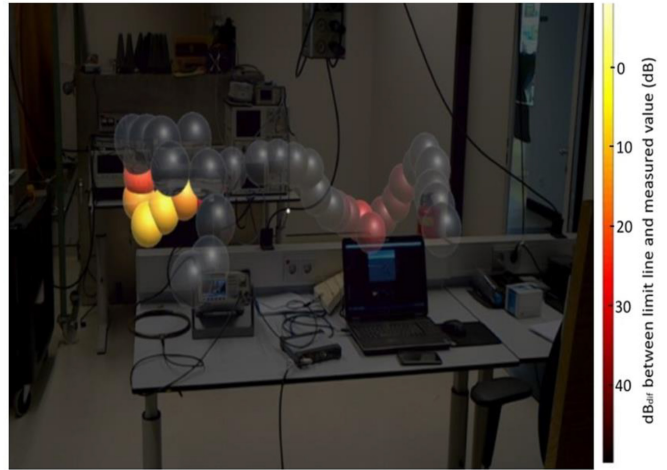


Fig. 8. Pinpointing the EM field spots in the office.

The bubbles at the top of the figure represent changes in the EM field above the EUT area, while the color changes at the bottom are not as pronounced due to the difference in EM levels between the two sources. The data presented in this figure underscores the capability of the proposed method to discern and precisely pinpoint the sources exhibiting peak EM field intensities. The color changes are most prominent near the box where a half-bridge board was placed, but the highest contrast between colors is observed in the top emission source since the limit line is not exceeded by this source.

Fig. 8 shows the measurement results obtained in an office setting, where a clear contrast is observed between areas with low EM levels (gray bubbles) and areas with high and medium EM levels (red and yellow). The yellow bubbles were measured near an antenna derived from a previous measurement, while the red bubbles were measured above a working laptop. The size of the bubbles can be adjusted to evaluate the measurement area more accurately. In this measurement, a bubble diameter of 13 cm was chosen, which was matched to the antenna diameter, and the distance between the centers of the bubbles was equal to half of the antenna diameter [8].

IV. CONCLUSION

Identifying the location of maximum emission, such as in the NRE01 test method, can be a significantly time-consuming process. To streamline this, we propose an AR-based measurement technique. This method leverages a digitizer, laptop, and AR glasses to deliver real-time insights into the field distribution around the EUT. By providing real-time feedback, this approach empowers test engineers to concentrate on regions of the highest emissions, thereby optimizing measurement time.

The system architecture involves a laptop that streams data to AR glasses via Wi-Fi and tracks the antenna’s position using a HoloLens device coupled with depth sensors. This innovative methodology promotes a flexible scanning path, mitigating the risk of overlooking any measurement positions and maintaining a visual connection with the data.

The versatility of the setup components allows for their substitution with equivalent alternatives to comply with various standards and requirements. The retention of measurement data post-test facilitates the generation of a 3-D map, enabling further examination of the EUT or test area. As postprocessing (FFT) data can be stored, the size of the scanning area or duration of testing becomes less critical, given the compactness of the data.

The proposed method functions as a prescan procedure for the equipment prior to the actual qualification measurements. When integrated with time-domain measurements, this prescan approach effectively evaluates the test area and pinpoints positions with elevated EM emission levels. This holistic and innovative process not only enhances the precision of measurements but also augments the efficiency of the overall testing process.

ACKNOWLEDGMENT

Great thanks to Mathon de Raad, a B.Sc. student from the University of Twente who was responsible for the Unity code for the AR glasses.

REFERENCES

- [1] *Technical Requirements for Electromagnetic Compatibility (EMC) Testing of Military Equipment and Systems*, AECTP Standard 501, Dec. 2016.
- [2] *American National Standard for Methods of Measurement of Radio-Noise Emissions from Low-Voltage Electrical and Electronic Equipment in the Range of 9 kHz to 40 GHz*, ANSI Standard C63.4, Jun. 2014.
- [3] *Specification for Radio Disturbance and Immunity Measuring Apparatus and Methods—Part 1–4: Radio Disturbance and Immunity Measuring Apparatus—Antennas for Conducted Disturbances and for Radiated Electromagnetic Field Measurements*, CISPR Standard 16-1-4:2019, Jan. 2019.
- [4] T. Hartman, N. Moonen, B. Ten Have, and F. Leferink, “Fast magnetic emission tests for continuous measurements around an equipment under test,” in *Proc. ESA Work. Aerosp. EMC, Aerosp.*, Aug. 2019, pp. 1–5.
- [5] J. Meng, X. Zhang, L. Zhang, and Z. Zhao, “Time-domain low-frequency non-periodic transient EMI measurement system,” *IET Sci. Meas. Technol.*, vol. 13, no. 5, pp. 650–655, Jul. 2019.
- [6] F. Krug and P. Russer, “The time-domain electromagnetic interference measurement system,” *IEEE Trans. Electromagn. Compat.*, vol. 45, no. 2, pp. 330–338, May 2003, doi: [10.1109/TEMC.2003.811303](https://doi.org/10.1109/TEMC.2003.811303).
- [7] C. Keller and K. Feser, “Fast emission measurement in time domain,” *IEEE Trans. Electromagn. Compat.*, vol. 49, no. 4, pp. 816–824, Nov. 2007, doi: [10.1109/TEMC.2007.908282](https://doi.org/10.1109/TEMC.2007.908282).
- [8] D. Pokotilov, R. Vogt-Ardatjew, and F. Leferink, “Continuous electromagnetic emission measurement setup with antenna position tracking,” in *Proc. Int. Symp. Electromagn. Compat. EMC EUROPE*, Nov. 2020, pp. 1–6, doi: [10.1109/EMCEUROPE48519.2020.9245689](https://doi.org/10.1109/EMCEUROPE48519.2020.9245689).
- [9] H. Nakamura and Y. Mizuno, “Development of augmented-reality-based magnetic field visualization system as an educational tool,” *Sensors*, vol. 22, no. 20, p. 8026, 2022. [Online]. Available: <https://doi.org/10.3390/s22208026>
- [10] R. Guarese, P. Andreasson, E. Nilsson, and A. Maciel, “Augmented situated visualization methods towards electromagnetic compatibility testing,” *Comput Graph.*, vol. 94, pp. 1–10, Feb. 2021, doi: [10.1016/j.cag.2020.10.001](https://doi.org/10.1016/j.cag.2020.10.001).
- [11] S. Matsumoto, K. Mitsufuji, Y. Hisasa, and S. Noguchi, “Real-time simulation method of magnetic field for visualization system with augmented reality technology,” *IEEE Trans. Magn.*, vol. 49, no. 5, pp. 1665–1668, May 2013.
- [12] D. G. B. van Rijswijk. “Visualisation of EMI in real-time.” Jul. 2021. [Online]. Available: <http://essay.utwente.nl/87774/>
- [13] “PicoScope 5000 series datasheet,” Data Sheet, Pico Technol. Ltd., St Neots, U.K., 2016. [Online]. Available: <https://www.picotech.com/download/datasheets/PicoScope5000SeriesDataSheet.pdf>